



# Thermodynamic and kinetic mechanisms in self-assembled quantum dot formation

Albert-László Barabási

*Department of Physics, University of Notre Dame, Notre Dame, IN 46556, USA*

Received 19 January 1999

## Abstract

Heteroepitaxial growth of highly strained structures offers the possibility to fabricate islands with very narrow size distribution, coined self-assembling quantum dots (SAQD). In spite of the high experimental interest, the mechanism of SAQD formation is not well understood. We will show that equilibrium theories can successfully predict the island sizes and densities, the nature and the magnitude of the critical thickness needed to be deposited for SAQD formation, as well as the onset of ripening. Furthermore, the flux and temperature dependence of the SAQDs is described using kinetic Monte Carlo simulations. © 1999 Elsevier Science S.A. All rights reserved.

*Keywords:* Thermodynamic mechanisms; Kinetic mechanisms; Self-assembled quantum dot

## 1. Introduction

Heteroepitaxial growth of highly strained structures has gained interest lately as it offers the possibility to fabricate nanoscale islands with very narrow size distribution. Such islands have been coined self-assembling quantum dots (SAQD). Although the understanding of the basic mechanisms determining the size and the distribution of the islands is hampered by the coexistence of equilibrium and nonequilibrium effects, equilibrium studies have been quite successful in capturing the key features of SAQD formation. The growth mode leading to strained island formation has been first proposed theoretically by Stranski and Krastanow as early as 1938, [1] and is now generally referred to as the Stranski–Krastanow (SK) growth mode. This mode of growth requires the deposition of several atomic layers of one material on the top of another of a different lattice constant under precisely controlled conditions. Due to the stringent requirements of such controlled thin layer deposition, the SK growth mode eluded the crystal growth community for a long time. Recent developments in epitaxial techniques, however, such as metal–organic chemical vapor deposition (MOCVD) and molecular beam epitaxy (MBE), have finally

made it possible to control layer deposition to the degree required by the SK process. By making the self-assembling processes possible, these advances have in effect opened a new era in nanostructure fabrication, making zero-dimensional geometries a very practical reality.

The highly reproducible features of QD formation have generated much interest in the theoretical community. In general, the theoretical work on self-assembly can be grouped into two classes: first, there is increasing evidence that many aspects of QD formation can be explained using energetic principles and *equilibrium* thermodynamics [2–5]. Second, since some properties of QD formation clearly exhibit nonequilibrium features, it is natural to invoke *dynamical* models and Monte Carlo (MC) simulations to further understand the mechanisms of island formation [6–9].

To fully understand heteroepitaxial island formation, we first need to describe the equilibrium thermodynamics of the system, which can serve as a starting point for the nonequilibrium analysis as well. Consequently, in the next section we discuss the equilibrium theory of self-assembled quantum dot formation. This will be followed by a discussion on nonequilibrium effects in Section 3. Finally, in Section 4 we will give a critical comparison between the equilibrium and

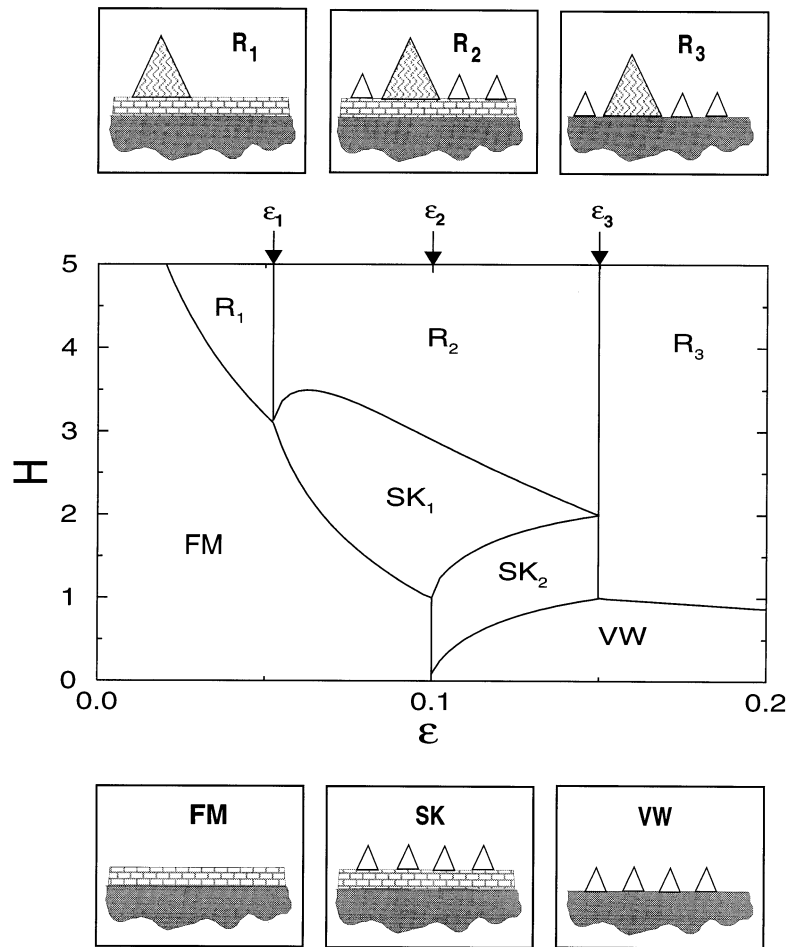


Fig. 1. Equilibrium phase diagram as a function of the coverage  $H$  and lattice misfit  $\epsilon$ . The small panels on the top and the bottom illustrate the morphology of the surface in the six growth modes. The small empty triangles indicate the presence of stable islands, while the large shaded ones refer to ripening islands. The phases are separated by the following phase boundary lines:  $H_{c_1}(\epsilon)$ : FM-R<sub>1</sub>, FM-SK<sub>1</sub>;  $H_{c_2}(\epsilon)$ : SK<sub>1</sub>-R<sub>2</sub>;  $H_{c_3}(\epsilon)$ : SK<sub>2</sub>-SK<sub>1</sub>;  $H_{c_4}(\epsilon)$ : VW-SK<sub>2</sub>, VW-R<sub>3</sub>. The parameters used to obtain the phase diagram are discussed in detail in Ref. [3].

nonequilibrium phenomena, and draw conclusions as to their relative roles.

## 2. Equilibrium theory of self-assembled QD formation

The equilibrium properties of strained heteroepitaxial systems — such as CdSe/ZnSe, Ge/Si, or InAs/GaAs — can be summarized in a phase diagram that not only predicts the main growth modes of various phases, but also provides a detailed characterization of these possible phases in terms of island density, equilibrium island size and, where applicable, the thickness of the wetting layer. In subsequent paragraphs we present the equilibrium model of dislocation-free island formation, followed by its predictions regarding the different growth modes [3,10].

### 2.1. Model description, free energy, and the phase diagram

In formulating the model, we consider that  $H$  mono-

layers of material A with lattice constant  $d_A$  are deposited on top of substrate B having a lattice constant  $d_B$ , and are allowed to equilibrate. Due to the lattice mismatch,  $\epsilon$ , defined by  $\epsilon = (d_A - d_B)/d_B$ , in equilibrium one expects that a certain fraction of the A atoms form a wetting film of  $n_1$  monolayers, and the rest of the material ( $H - n_1$  monolayers) is distributed in the form of 3D islands. We assume that the 3D islands have a pyramidal shape with a fixed aspect ratio, corresponding to a single energy minimum, as conventionally given by Wulff's plot [11]<sup>1</sup>. Neglecting evaporation, the deposited material represents a conserved system that is in equilibrium with a thermal reservoir. Thus the relevant thermodynamic potential density is the free-energy per atom,  $f = u - Ts$ , where  $u$  is the internal energy density,  $T$  is the temperature, and  $s$  is the entropy density of the system. To obtain the equilibrium prop-

<sup>1</sup> In fact the Wulff plot can have multiple minima, but this simplification makes the model tractable without significantly changing the equilibrium properties of the model.

erties of this system, we have to minimize  $f$  with respect to the wetting film thickness ( $n_1$ ), the total mass accumulated in the island, and the equilibrium island size. The growth modes (phases) provided by such a minimization process as a function of the two most relevant experimental parameters — the amount of the material deposited  $H$ , and the lattice misfit  $\epsilon$  — are summarized in the phase diagram shown in Fig. 1. An absolute minima of the free energy at nonzero island size indicates the existence of finite stable islands. If the asymptotic value of the free energy (for large islands) is smaller or equal to the minimum corresponding to finite islands, ripening takes place in the system. In the following we discuss the properties of the phases predicted by the analysis, as shown by the phase diagram.

### 2.1.1. The FM phase

In this phase, the deposited material contributes to the pseudomorphic growth of the wetting film, and the islands are absent, reminiscent of the so-called Frankvan der Merwe (FM) growth mode. The wetting layer thickness in this case is the same as the nominal thickness of the material deposited,  $H$ . Such growth of the wetting layer will continue until  $H$  reaches a critical value  $H_{c_1}(\epsilon)$ , which defines the phase boundary between the FM and either the  $R_1$  or the  $SK_1$  phases, as shown in Fig. 1.

### 2.1.2. The $R_1$ Phase

Above  $H_{c_1}(\epsilon)$ , but when the inequality  $0 < \epsilon < \epsilon_1$  is satisfied after the formation of a wetting layer of  $n_1 = H_{c_1}(\epsilon)$  monolayers, the excess material ( $H - n_1$ ) contributes to the formation of *ripening* islands.

### 2.1.3. The $SK_1$ phase

Above  $H_{c_1}(\epsilon)$ , and for  $\epsilon_1 < \epsilon < \epsilon_2$ , the deposited material  $H$  is distributed between the wetting film, and finite stable islands, in a process similar to the Stranski–Krastranow (SK) growth mode. At  $H_{c_1}(\epsilon)$  the equilibrium island size *jumps* from zero (in the FM phase) to some finite  $x_0(H, \epsilon)$  value. Naturally, within the  $SK_1$  phase the island size, their mass, the wetting layer thickness, and the island density  $\rho$  are continuous functions of  $H$  and  $\epsilon$ . With increasing  $H$ , the density  $\rho$  increases from 0 at  $H_c$  to a finite value. Interestingly, as a consequence of island–island interactions in the  $SK_1$  phase the wetting layer also continues to grow, but at a sub-linear rate.

### 2.1.4. The $R_2$ phase

In this phase the deposited material  $A$  is distributed between a wetting film, finite islands, and ripening islands. The finite islands formed in the  $SK_1$  phase are preserved, being stable with respect to ripening. Thus in the  $R_2$  phase both finite stable islands and ripening islands coexist.

### 2.1.5. The VW phase

For large lattice misfits ( $\epsilon > \epsilon_2$ ) and for small coverages  $H$ , all the deposited material is accumulated in the form of finite islands. Due to the large misfit, in this phase the wetting film is absent and the islands form directly on the substrate, similar to the so-called Volmer–Weber (VW) growth mode. In the absence of the wetting film, both the island size  $x_0$  and the island density  $\rho$  simply increase with  $H$ .

### 2.1.6. The $SK_2$ phase

By increasing  $H$  in the regime  $\epsilon_2 < \epsilon < \epsilon_3$  we reach a new phase when  $H$  exceeds the value  $H_{c_4}(\epsilon)$ , which we label the  $SK_2$  phase. In this phase the behavior of the system is quite different from the  $SK_1$  growth mode, since at the  $H_{c_4}$  boundary we already have islands formed in the  $VW_4$  mode. As we enter the  $SK_2$  phase by increasing  $H$  above  $H_{c_4}$ , the island density and the island size remain unchanged, but a wetting film starts to form. This process continues until a full monolayer is completed, at which point we enter the  $SK_1$  phase. Thus, in contrast with the  $SK_1$  phase, in the  $SK_2$  phase the formation of new islands is suppressed until the one-monolayer-thick wetting layer is completed.

### 2.1.7. The $R_3$ phase

In this last phase, which occurs for  $\epsilon > \epsilon_3$  and for  $H > H_{c_3}$ , we expect the formation of ripening islands. The formation of stable islands is suppressed, and all the material deposited after  $H_{c_3}$  contributes only to the formation of new *ripening* islands, that *coexist* with the stable islands which had been formed in the VW growth mode. However, in contrast with  $R_2$ , in the  $R_3$  phase the wetting film is absent.

## 2.2. Comparison with experiment

A quantitative comparison of the phase diagram with experiment requires the knowledge of materials parameters which determine the values of  $\epsilon_1$ ,  $\epsilon_2$ ,  $\epsilon_3$ , and the location of the boundaries in the phase diagram. We have shown that allowing for all possible values of the material constants that enter in the free energy, there are four topologically distinct phase diagrams, but none of the three new diagrams contain new phases [10].

The formation of the pseudomorphic wetting layer for small  $H$  and  $\epsilon$  has been documented in various systems (including the CdSe/ZnSe system of interest here) [12], being a general feature of strained layer formation. Also, experiments have shown that the transition from the FM to the  $SK_1$  phase is independent of the deposition rate [13], indicating that its origin is thermodynamic rather than dynamic. Furthermore, recent investigations have measured the strain dependence of  $H_{c_1}$ , indicating that the critical wetting layer

thickness decreases with increasing lattice misfit [14], in agreement with the decreasing tendency of the  $H_{c_1}$  phase boundary seen on the left-hand-side of Fig. 1.

After the critical thickness has been reached, rapid formation of uniform islands is observed in a variety of materials [15–17]. The behavior of the free energy at  $H_{c_1}$  allows us to identify the nature of this transition: it corresponds to the appearance and a slow shift of a lower minimum in the free energy — a typical signal for a *second order phase transition* in the system [18]. Furthermore, we find that in the close vicinity of  $H_{c_1}$  the island density  $\rho$  increases linearly with  $(H - H_{c_1})$ . However, when  $(H - H_{c_1})$  becomes larger, the island–island interactions lead to a sub-linear increase in the density. Indeed, in the InAs/GaAs system investigated by Miller et al. [19–21] it was found that, after stopping deposition, the system first went through a transient regime, after which it equilibrated. The *equilibrated* island density then *increased linearly* with coverage, in agreement with our prediction stated above.

In the discussion of the transition from the FM to the  $R_1$  regime we noted that, unlike the island density  $\rho$ , the equilibrium island size does not increase continuously near  $H_{c_1}$ , but *jumps discontinuously* from 0 to  $x_0$  ( $\epsilon$ ,  $H_{c_1}$ ). This is again in agreement with experiment since — once the islands form — they reach a well defined size, small islands being rather rare [15,22,16,17]. The experiments also indicate that, although an increasing  $H$  does result in some modification of the equilibrium island size, this change is not significant, most of the newly deposited material contributing to the formation of *new* islands [15–17], again in agreement with a *slowly changing* value of  $x_0$  and a *rapidly* increasing  $\rho$ .

Finally, the phase diagram indicates that the stability of the islands depends on the coverage  $H$ . For example, for sufficiently large coverages ripening should take place in the system independent of the value of  $\epsilon$ . Ripening has been demonstrated convincingly in two systems: Ge on Si [4,23] and CdSe on ZnSe [24]. The CdSe/ZnSe system manifests the ripening process in a striking way, at a rate and a scale that is particularly convenient to follow by AFM measurements. Repeated AFM scans of *the same sample area* at 48 h intervals have provided evidence that the dots evolve in both diameter and height as time progresses, fully consistent with the predictions of Ostwald ripening [25–27]: large islands grow by accumulation of material from smaller islands, diffused along the substrate. Furthermore, when the trends in the island ripening have been extrapolated back, the islands converged at approximately one value of the diameter, strongly suggesting that the CdSe dots are really quite uniform at the moment of formation. Finally, the island density has been found to decrease as  $\rho(t) \sim t^{-1}$  in excellent agreement with predictions of strain free Ostwald ripening for interface-transfer-mediated growth [25,26].

These results allow us to identify the growth regime in which the self-assembled QDs are formed in the CdSe/ZnSe system, in light of the equilibrium theories of growth [3], as summarized in the phase diagram in Fig. 1. The experimental results, demonstrating that CdSe/ZnSe islands begin to form only after the deposition of 2.5–3.0 ML of CdSe, clearly argue for the formation of a CdSe wetting layer, thus excluding the VW growth mode; and since the observed islands are not stable in time, the SK mode can be excluded as well. Rather, the experimental results indicate a direct transition from the wetting film to islands that ripen, a transition that is predicted by the equilibrium growth theory labeled as  $R_1$  in the phase diagram in Fig. 1.

Having made this conclusion, the remarkable uniformity of the islands just when the growth process stops may at first be puzzling. A closer look at the equilibrium theory indicates, however, that such uniformity at the transition from the 2D growth to ripening is indeed to be expected. The existence of a stage characterized by uniform islands requires the existence of a metastable minimum in the free energy function as a function of volume. When strain is included in the calculations, the resulting free energy of the strained QD system [3] indeed does predict the existence of such a metastable minimum at the 2D-to-ripening transition. The presence of this relative minimum modifies the growth process (without modifying the equilibrium state of the system) by *temporarily* trapping the islands. The nucleated islands are then *small* and *uniform*, and — in order to ripen — they must first escape from the metastable state.

### 3. Dynamical theory of self-assembled QD formation

For homoepitaxial systems many details of the island formation process have been clarified using atomistic models and numerical simulations [28]. In heteroepitaxy the mobility of an atom is determined not only by the *local* bonding energies (essentially ‘chemistry’), but also by the *nonlocal* strain field. Since strain depends on the full surface morphology and composition, modeling growth in a strained system at the atomic level is very computer-time-intensive. Nevertheless, a number of recent studies have pioneered various Llonde Carlo methods to study heteroepitaxial growth [6–8].

In our own investigation of the epitaxial growth process, we have recently performed simulations designed to help uncover the mechanism of self-assembled QD formation [9]. The one-dimensional model used by us includes all microscopic elements common to the materials for which QD formation has been observed, namely, deposition rate, activated diffusion, and strain relaxation at *every* deposition and diffusion event. When 2 ML of a material with a lattice constant  $a_A^0$  are

deposited on a substrate with a lattice constant  $a_B^0$ , we find that self-assembled islands will form as long as the misfit  $\epsilon$  is sufficiently large.

The most convincing evidence of the stress-induced self-assembling process is provided by the island size distribution shown in Fig. 2. For  $\epsilon = 0$  and 2.5% (i.e. much below the CdSe/ZnSe case, of interest in this chapter) the distribution is wide; i.e. the system contains islands of all sizes, with a small peak around the island size  $s = 20$ . However, for  $\epsilon = 5$  and 7.5% (which includes the CdSe/ZnSe and its sister III-V combination, InAs/GaAs), the distribution has a *narrow peak* centered at  $s = 6$  for  $\epsilon = 5\%$ , and at  $s = 5$  for  $\epsilon = 7.5\%$ .

The parameter capturing the dynamics of self-assembly in the system is the parameter  $w_s/\bar{s}$ , shown in Fig. 2, where  $w_s^2 \equiv \bar{s}^2 - \bar{s}^2$  is the width of the island size distribution and  $\bar{s}$  is the average island size. We can refer to  $w_s/\bar{s}$  as the *relative width*. An increasing  $w_s/\bar{s}$  indicates unbounded growth of fluctuations, while a *decreasing* relative width is a signal of self-organization in the system. As Fig. 2 indicates, for  $\epsilon = 0$  and 2.5%  $w_s/\bar{s}$  increases continuously with coverage, while for  $\epsilon = 5$  and 7.5% the parameter  $w_s/\bar{s}$  increases only until it reaches a peak at some small coverage  $H_c$ , after which it decays. The presence of the peak signals the onset of self-organization: for  $H > H_c$  we witness a continuous increase in the *uniformity* of the island size.

### 3.1. Mechanism of self-organization

The main difference between the dynamical properties of stress-free and stressed systems comes in two strain-related effects, that we discuss separately [9].

(a) First, strain lowers the energy barrier for diffusion, thus making diffusive hops more probable. Fig. 3 shows the strain energy in the vicinity of an island for  $\epsilon = 7.5\%$ , indicating that the *substrate is strained* and that the strain energy,  $E_s$ , decreases as we move away from the edge of the island. This means that if atoms are deposited near an island, strain will *bias* their otherwise random motion, generating a net surface current  $\mathbf{j} = -\nabla\mu(x)$ , where  $\mu(x)$  is the local chemical potential [28]. The only contribution to such current comes from the position-dependence of the strain energy, leading to  $\mathbf{j} \simeq -\nabla E_s$ , that points towards the decreasing strain direction. Thus the strain field around an island generates a *net current of adatoms away from the island*.

(b) And second, for large islands the strain energy  $E_s$  at the island edge becomes comparable to the bonding energy of the edge atom, enhancing its detachment, and thus leading to a gradual dissolution of the island. Such a mechanism favors a smaller average island size, and leads to a narrower island size distribution, as demonstrated by numerical simulation of Ratsch et al. [8].

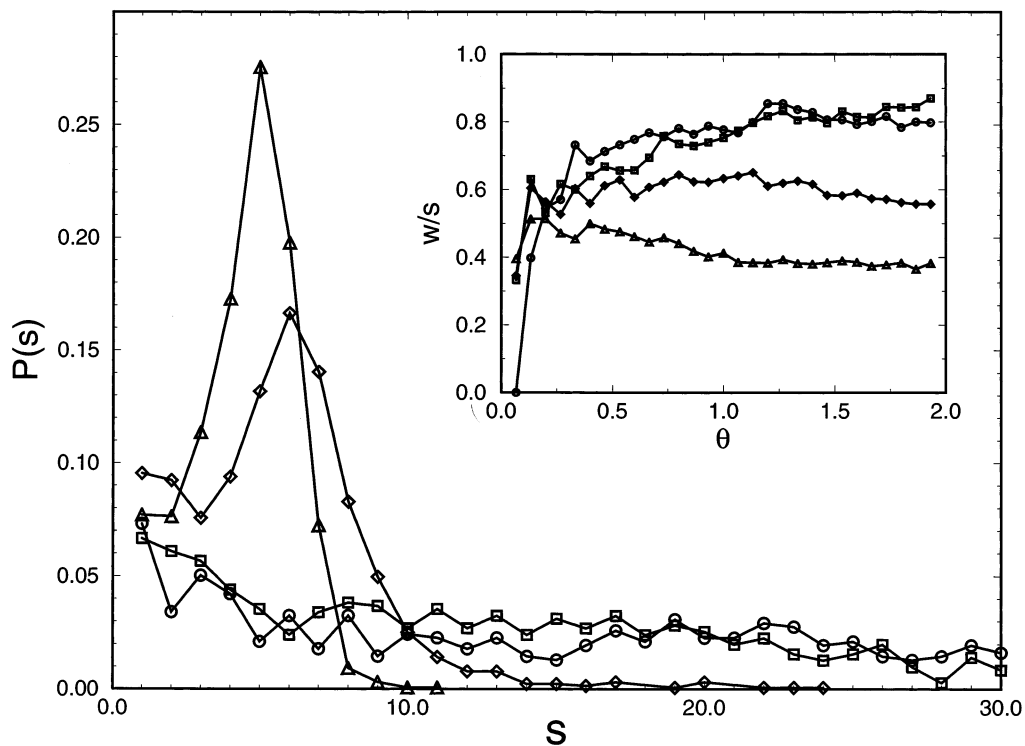


Fig. 2. (a) Island size distribution measured after the deposition of 2ML of material A. Inset: Relative width  $w_s/\bar{s}$  as a function of coverage. The symbols correspond to misfit values 0% ( $\circ$ ), 2.5% ( $\square$ ), 5% ( $\diamond$ ), and 7.5% ( $\triangle$ ).

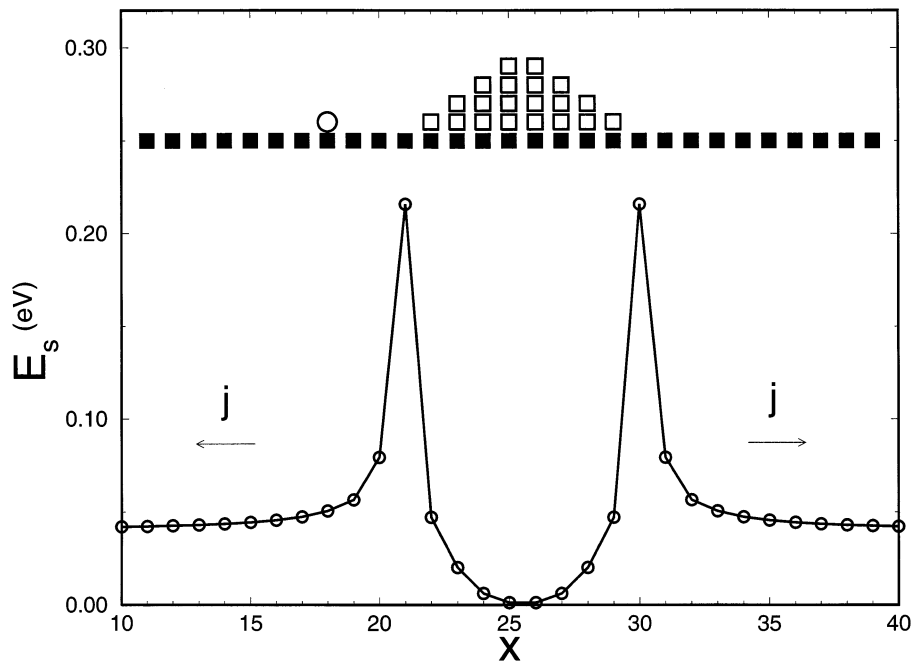


Fig. 3. Strain energy profile around a typical island. The substrate (■) and the islands on top of it (□) are shown in the upper part of the figure.  $E_s$  is the strain energy of an atom placed on top of the substrate or on the island. For example,  $E_s$  at  $x = 18$  is the strain energy felt by the adatom shown by the circle on top of the substrate. One can see that  $E_s$  is the largest when the atom is at the edge of the island ( $x = 21, 30$ ).  $E_s$  decays as the adatom moves away from the island, generating a net current,  $j(x)$ , shown by the arrows. Note that  $E_s$  does not decay to zero, since the monomer can locally stretch the substrate.

The simultaneous action of (a) and (b) thus leads to a kinetic mechanism that stabilizes the island size: as islands grow, a strain field develops, tending to *detach* the edge atoms (effect (b)) and to *push* them away from the islands (effect (a)). Furthermore, the newly deposited atoms also diffuse away from the larger islands (effect (a)). These combined effects *slow the growth rate of large islands* and *increase the adatom density* away from them, thus *enhancing the nucleation of new islands*. The newly nucleated islands are small, and so is the strain field around them, so that they grow at a much faster rate than the older, larger islands. This eventually results in a narrow island size distribution in the system (Fig. 2a). However, it is important to note that the two discussed kinetic mechanisms (a and b) are not alone in stabilizing the island sizes: they act together with the equilibrium considerations discussed in Section 2. A more detailed discussion on the interplay between equilibrium and nonequilibrium effects will be offered the next section.

#### 4. Equilibrium versus nonequilibrium theory: the limits of applicability

After this review of the equilibrium (Section 2) and the nonequilibrium theories (Section 3), we have to pause and ask the question: which of the two mechanisms is responsible for self-assembled island formation

in the experimentally relevant systems? There is no simple answer to this question, and we believe that most experiments display *both* equilibrium and nonequilibrium effects. The question is whether one can combine the two mechanisms to provide a satisfactory description of strained island formation, such as CdSe QDs on ZnSe. The following plausible picture emerges regarding the mechanism of self-assembled island formation. For QD formation carried out at very small fluxes, one expects that most features will agree with the equilibrium predictions. However, since most growths are done at some finite flux, the system is *never completely equilibrated*, and the equilibrium features are often suppressed by nonequilibrium effects. We believe that the existence of the wetting layer is an equilibrium feature of the system, which is robust enough to dominate even in strong nonequilibrium conditions. However, growth at a high flux or at a low temperature (or both) can easily lead to the overgrowth of the wetting layer, delaying the onset of island formation [15]. Upon annealing, however, such an overgrown wetting layer should lose most of its excess material, the atoms being rearranged to form strained islands as they tend toward equilibrium. [4,23]. This has indeed been observed in numerous materials, including CdSe/ZnSe [12].

Once islands begin to form, they will grow towards the size predicted by the equilibrium theory. However, islands nucleate randomly, first forming islands of

monolayer thickness (submonolayer coverage), which later become three-dimensional. The mechanism and the energetics of the shape transition is just in the process of being understood [29–31], and it is likely that this aspect is system-dependent as well. Since the initial monolayer-thick island formation — both island size and island density — is clearly sensitive to both flux and temperature [28], one expects that this nucleating process will have a dynamic character, that can be described by Monte Carlo simulations. As islands continue to grow, strain effects become relevant. It is only at this point that the islands begin to approach the size and density predicted by the equilibrium theory. However, even at this stage the process is slowed down by nonequilibrium mechanism discussed in Section 3: as the size of an island increases, it becomes increasingly difficult for new atoms to attach themselves to the island due to biased diffusion (see Fig. 3) and to detachment of atoms from the edges. The random nucleation of monolayer islands at the initial submonolayer coverage, as well as size-limiting dynamical processes are responsible for the experimentally observed dependence of the island size and density on flux and temperature. [16,17] One expects that, as the flux is decreased, the system approaches the equilibrium configuration, and thus the island size and density will both saturate.

A beautiful demonstration of the above ideas is available for Ge quantum dots grown on Si(001) substrate [4,23,22], a system with relative strain of 0.025, not so different from the 7% mismatch of CdSe/ZnSe. As the system is annealed, the island size distribution approaches a saturation value, corresponding to the equilibrium configuration. Although partially annealed configurations show rather strong nonequilibrium features, once they are fully annealed, the size distribution of the islands is in excellent agreement with the predictions of the equilibrium theory.

## 5. Outlook

The interplay between the equilibrium and non-equilibrium approaches does offer a good starting point for a comprehensive theory of SAQD formation. Naturally, as with every theory, the conclusions do depend on the assumptions made during the construction of the free energy. However, as more and more details of SAQD formation are being elucidated, new phenomena emerge that were not considered and incorporated in the previous approaches. Next we discuss some of these problems, and outline shortly the difficulties involved in their solution.

First, the equilibrium theory assumed that there is only one type of island present in the system. However, most prominently for SiGe, there is evidence of multi-

ple island shapes and transitions between them. Energetic principles can be generalized to address the nature and the origin of these shape transitions [29], giving results that are in good qualitative agreement with the experiments. Second, the free energy discussed here does not allow for composition modulations during SAQD formation. However, there is rather convincing evidence for both group IV and III-V materials that at high temperatures considerable alloying takes place. It is possible to generalize the equilibrium theories to address these questions [32], but a new phase diagram incorporating the effects of alloying is not available yet. Finally, a question of considerable importance is the ordering of the SAQDs. Such ordering process might lead to even narrower size distributions, a highly coveted goal for electronic applications. Such ordering is a topic of high interest, but a better understanding of the nucleation process is needed to obtain significant progress in this directions. Possibilities include nucleation induced on prepatterned surfaces [33], that has been shown to lead to improvements in the QD sizes.

## Acknowledgements

We wish to acknowledge discussions with I. Daruka, J.K. Furdyna, H. Jeong, and C.S. Lee, who have greatly contributed to the results summarized in this paper. This research was supported by ONR YI program.

## References

- [1] I.N. Stranski, L. Krastanow, *Sitzungsber. Akad. Wiss. Wien, 'Zur Theorie der orientation Ausscheidung von Ionenkristallen aufeinander'*, *Math.-Naturwiss. K1 Abt. IIB* 146 (1938) 797.
- [2] V.A. Shchukin, N.N. Ledentsov, P.S. Kopev, D. Bimberg, *Phys. Rev. Lett.* 75 (1995) 2968.
- [3] I. Daruka, A.-L. Barabási, *Phys. Rev. Lett.* 79 (1997) 3708.
- [4] G. Medeiros-Ribeiro, A.M. Bratkovski, T.I. Kamins, D.A.A. Ohlberg, R.S. Williams, *Science* 279 (1998) 353.
- [5] D. Jesson, K.M. Chen, S.J. Pennycook, T. Thundat, R.J. War-mack, *Phys. Rev. Lett.* 77 (1996) 1330.
- [6] B.G. Orr, D. Kessler, C.W. Snyder, L.M. Sander, *Europhys. Lett.* 19 (1992) 33.
- [7] T.T. Ngo, P.M. Petroff, H. Sakaki, J.L. Merz, *Phys. Rev. B* 53 (1996) 9618.
- [8] C. Ratsch, A. Zangwill, P. Smilauer, *Surf. Sci.* 314 (1994) L937.
- [9] A.-L. Barabási, *Appl. Phys. Lett.* 70 (1997) 2565.
- [10] I. Daruka, A.-L. Barabási, *App. Phys. Lett.* 72 (1998) 2102.
- [11] G. Wulff, *Z. Kristallogr.* 34 (1901) 449.
- [12] H. Kirmse, R. Schneider, M. Rabe, W. Neumann, F. Henneberger, *Appl. Phys. Lett.* 72 (1998) 1329.
- [13] J.-M. Gerard, in: E. Burstein, C. Weisbuch (Eds.), *Confined Electrons and Photons*, Plenum Press, New York, 1995.
- [14] G. Abstreiter, et al., *Semic. Sci. Tech.* 11 (1996) 1521.
- [15] P.M. Petroff, G. Medeiros-Ribeiro, *MRS Bulletin* 21 (No 4), 50, 1996.

- [16] W. Seifert, N. Carlsson, M. Miller, M.-E. Pistol, L. Samuelson, L. Wallenberg, *J. Crystal Growth Charact. Mater.* 33 (1996) 423.
- [17] R. Nötzel, *Semicon. Sci. Technol.* 11 (1996) 1365.
- [18] H.E. Stanley, *Introduction to Phase Transitions and Critical Phenomena*, Oxford University Press, New York, 1971.
- [19] D. Leonard, K. Pond, P.M. Petroff, *Phys. Rev. B* 50 (1994) 11687.
- [20] M.S. Miller, S. Jeppesen, D. Hessman, B. Kowalski, I. Maximov, B. Junno, L. Samuelson, *Solid-State Electr.* 40 (1996) 609.
- [21] N.P. Kobayashi, T.R. Ramachandran, P. Chen, A. Madhukar, *Appl. Phys. Lett.* 68 (1996) 3299.
- [22] T.I. Kamins, E.C. Carr, R.S. Williams, S.J. Rosner, *J. Appl. Phys.* 81 (1997) 211.
- [23] F.M. Ross, J. Tersoff, R.M. Tromp, *Phys. Rev. Lett.* 80 (1998) 984.
- [24] S. Lee, I. Daruka, C.S. Kim, A.-L. Barabási, J.L. Merz, J.K. Furdyna, *Phys. Rev. Lett.* 81 (1998) 3479.
- [25] W. Ostwald, *Z. Phys. Chem. (Leipzig)* 34 (1990) 495.
- [26] M. Zinke-Allmang, et al., *Surf. Sci. Rep.* 16 (1992) 377.
- [27] M. Zinke-Allmang, L.C. Feldman, M.H. Grabow, *Surf. Sci. Rep.* 16 (1992) 377.
- [28] A.-L. Barabási, H.E. Stanley, *Fractal Concepts in Surface Growth*, Cambridge University Press, Cambridge, 1995.
- [29] I. Daruka, J. Tersoff, A.-L. Barabási, *Phys. Rev. Lett.* 82 (1999) 2753.
- [30] T.J. Drucker, *Phys. Rev. B* 48 (1993) 18203.
- [31] C. Priester, M. Lannoo, *Phys. Rev. Lett.* 75 (1995) 93.
- [32] J. Tersoff, *Phys. Rev. Lett.* 81 (1998) 3183.
- [33] C. Lee, A.-L. Barabási, *Appl. Phys. Lett.* 73 (1998) 2651.